Supplemental Figure 1. CD8$^+$ and DN γδ T cell subsets respond to early *Mycobacterium tuberculosis* infection. (a) γδ T cell abundance among T cells in community controls (green) and contacts (purple). Color coding applies to all panels. Data in all panels represent mean +/- SD. (b) TCRγδ staining in CD8$^+$ T cells and (c) DN T cells. (d) CD8$^+$ γδ T cell activation measured by CD69 staining at rest (left) or after anti-CD3/CD28 activation (right) with IGRA stratification. (e) CD8$^+$ γδ T cell activation/exhaustion measured by PD-1 staining at rest (left) or after anti-CD3/CD28 (right) with IGRA stratification. (f) DN γδ T cell CD69 staining and (g) PD-1 staining at rest (left) or after anti-CD3/CD8 (right) with IGRA stratification. Groups were compared by unpaired t-test with significance level of $p<0.05$.*$p<0.05$ **$p<0.005$ IGRA: interferon γ release assay

Supplemental Figure 2. Lack of iNKT response during early *Mycobacterium tuberculosis* infection. (a) Density plots demonstrating the gating strategy for iNKT cells: left panel is gated on live CD3$^+$ cells and right panel is gated on iNKT cells. (b) iNKT abundance among T cells in community controls (green) and contacts (purple). Color coding applies to all panels. Data in panels b-f represent mean +/- SD. (c) iNKT subset abundance among their respective T cell subset. (d) Relative abundance of iNKT subsets among iNKT cells. (e) iNKT subset activation measured by CD69 staining at rest (left) or after anti-CD3/CD28 activation (right). (f) iNKT subset activation/exhaustion measured by PD-1 staining at rest (left) or after anti-CD3/CD28 (right). Groups were compared by unpaired t-test with significance level of $p<0.05$. *$p<0.05$

Supplemental Figure 3. MR1-5OPRU tetramers specifically stain MAIT cells. Panels a-c are representative flow cytometric dot plots from one healthy Haitian donor gated on live CD3$^+$ cells comparing staining of MAIT cells with MR1-5OPRU tetramers (left) or MR1-6FP tetramers (right) in the resting (a), 5ARU/MeG (b) or anti-CD3/CD28 conditions (c). (d) Bar graphs representing mean %MAIT cells of CD3$^+$ cells +/- SD in five healthy Haitian donors over three conditions.

Supplemental Figure 4. Representative flow cytometric plots of MAIT cell activation markers. (a) Dot plots gated on live CD3$^+$ cells identifying MAIT cells as tetramer$^+$CD161^{++} cells after 15 hrs of rest (left), 5ARU/MeG (middle) or anti-CD3/CD28 stimulation (right). Stimulation conditions apply to all plots within the panel column. Panels b-e are contour plots gated on the respective MAIT cell population indicated in the same column of panel (a) and demonstrate

gating strategies for activation markers CD69 (b), CD25 (c), GzB (d), and IFNγ (e). GzB: granzyme B; IFNγ: interferon γ

Supplemental Figure 5. DN MAIT cells are relatively enriched in contacts but do not demonstrate an activation phenotype. (a) DN MAIT cell abundance among DN T cells in community controls (green) and contacts (purple). Color coding applies to all panels. Data in all panels represent mean +/- SD. (b) DN MAIT cell abundance among MAIT cells at rest and after 5ARU/MeG activation. (c) DN MAIT cell abundance among MAIT cells stratified by IGRA status at rest (left) or after 5ARU/MeG (right). (d) DN MAIT cell activation measured by CD69 staining at rest or after 5ARU/MeG. (e) DN MAIT cell activation/exhaustion measured by PD-1 staining at rest or after 5ARU/MeG. (f) DN MAIT cell activation measured by CD25 staining at rest and after 5ARU/MeG. Groups were compared by unpaired t-test with significance level of $p<0.05$. *$p<0.05$ IGRA: interferon γ release assay

Supplemental Figure 6. Spearman correlation scatter plots of 16SrDNA OTU and innate-like T cell abundance/function demonstrate associations between microbial constituents and innate-like T cell immunity. All OTUs with relative abundance that significantly different between controls and contacts ($p<0.01$; Fig 5b) were correlated with immune phenotypes that were also significantly different between groups ($p<0.05$; Fig 1, 3). Relative abundance of OTU (y axis) was plotted against the relevant immune phenotype value with linear regression line representing the direction of correlation.

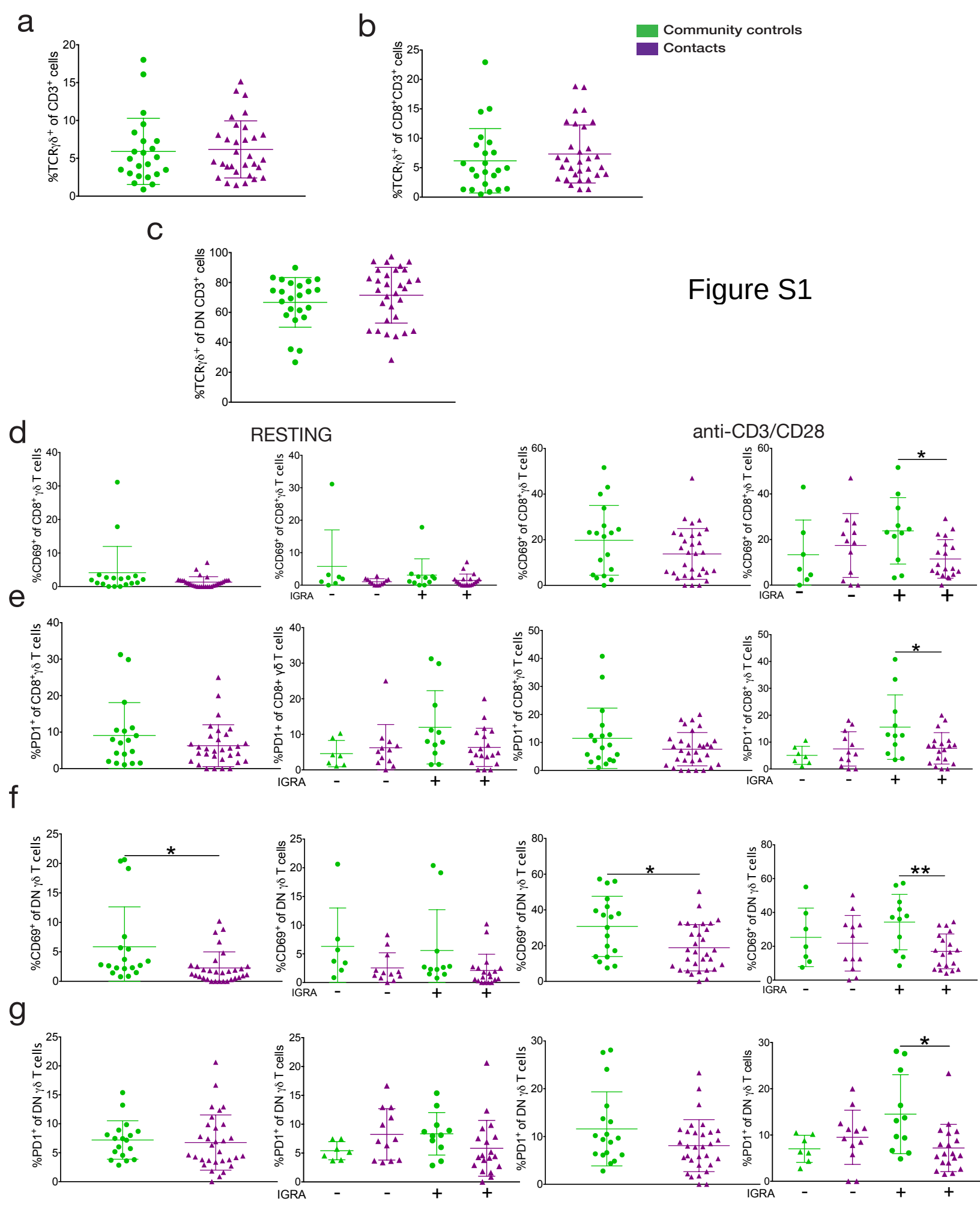
a
b
c
d
e
f
g
Community controls
Contacts
%TCRγδ+ of CD3+ cells
%TCRγδ+ of CD8+CD3+ cells
%TCRγδ+ of DN CD3+ cells
RESTING
anti-CD3/CD28
%CD69+ of CD8+γδ T cells
%PD1+ of CD8+γδ T cells
%PD1+ of CD8+ γδ T cells
%CD69+ of DN γδ T cells
%PD1+ of DN γδ T cells
IGRA
- - + +
*
**

Figure S1

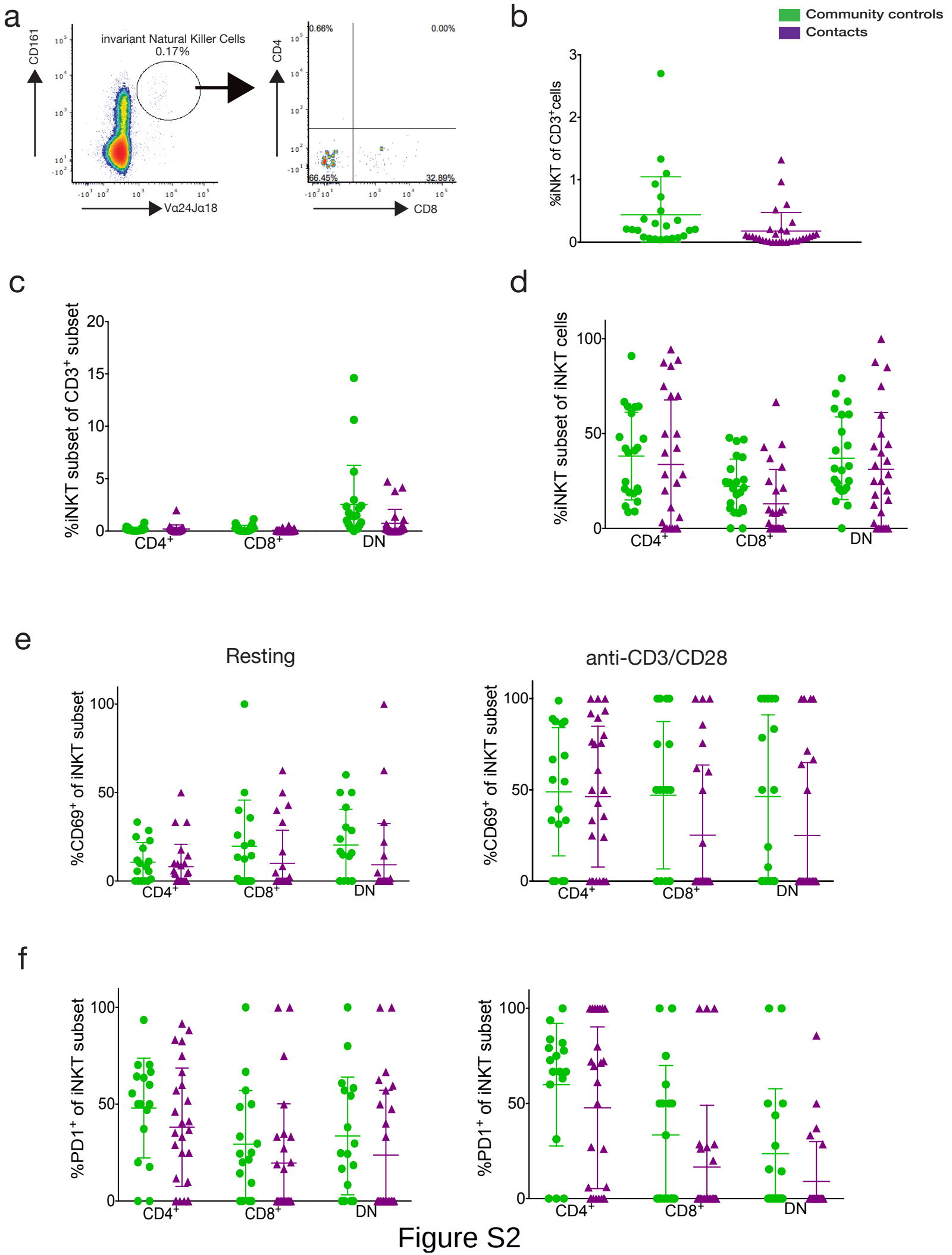
a
CD161
invariant Natural Killer Cells
0.17%
Vα24Jα18
CD4
0.66%
0.00%
66.45%
32.89%
CD8
b
Community controls
Contacts
%iNKT of CD3+cells
c
%iNKT subset of CD3+ subset
CD4+
CD8+
DN
d
%iNKT subset of iNKT cells
CD4+
CD8+
DN
e
Resting
anti-CD3/CD28
%CD69+ of iNKT subset
CD4+
CD8+
DN
f
%PD1+ of iNKT subset
CD4+
CD8+
DN

Figure S2

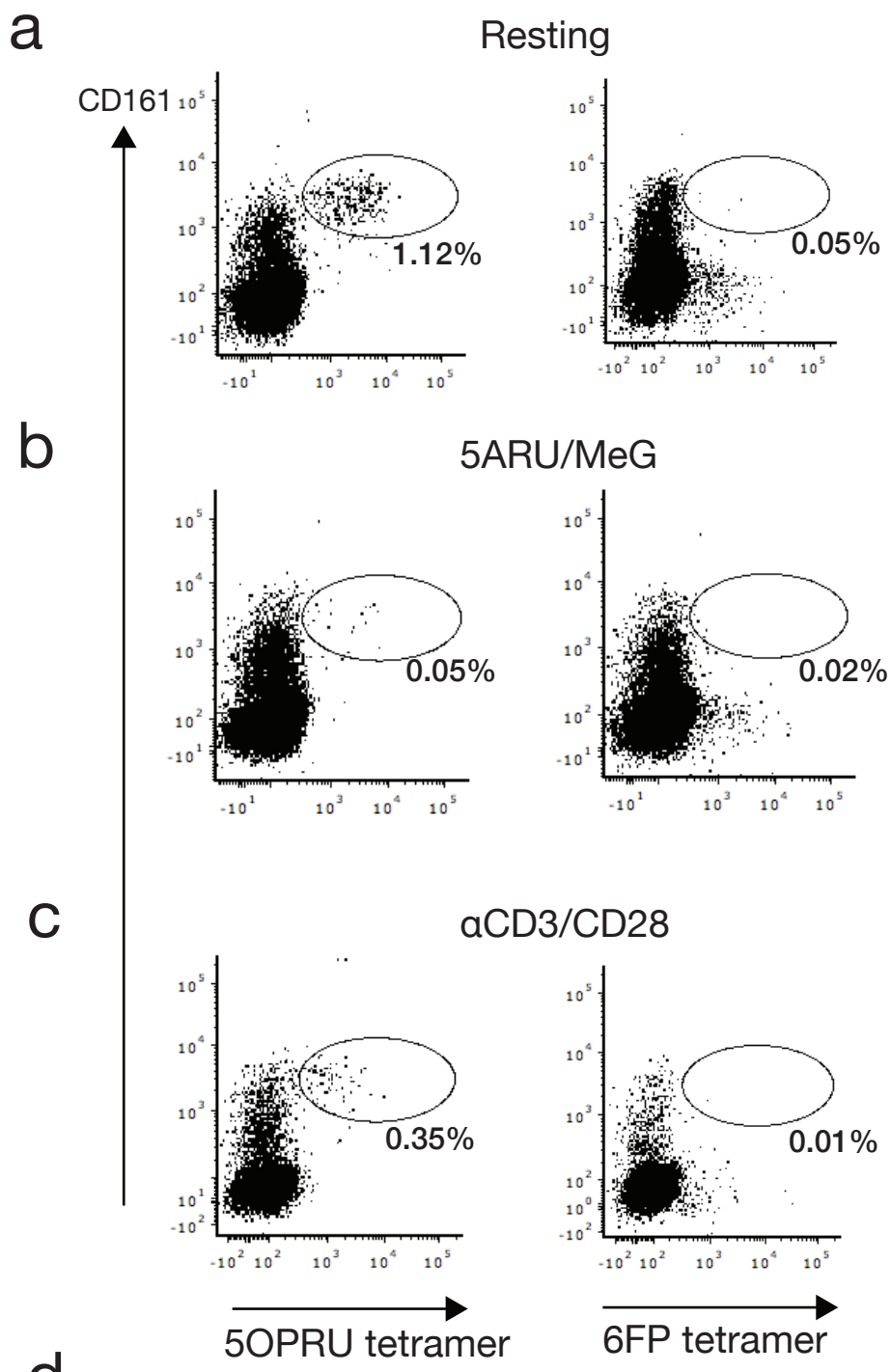
a
Resting
CD161
1.12%
0.05%
b
5ARU/MeG
0.05%
0.02%
c
αCD3/CD28
0.35%
0.01%
5OPRU tetramer
6FP tetramer

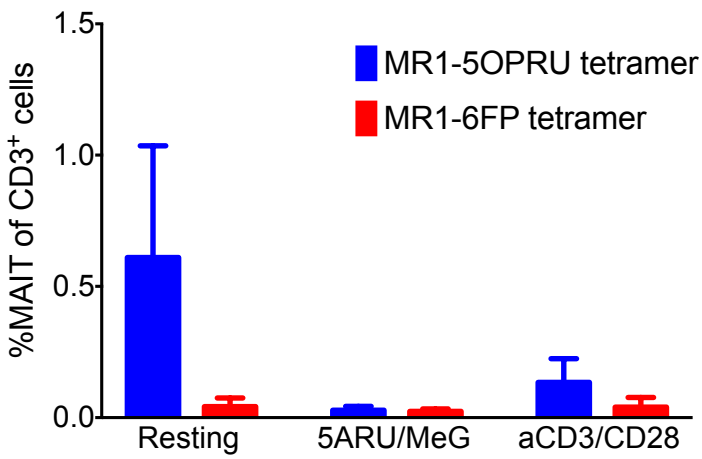
d
%MAIT of CD3+ cells
1.5
1.0
0.5
0.0
MR1-5OPRU tetramer
MR1-6FP tetramer
Resting
5ARU/MeG
aCD3/CD28

Figure S3

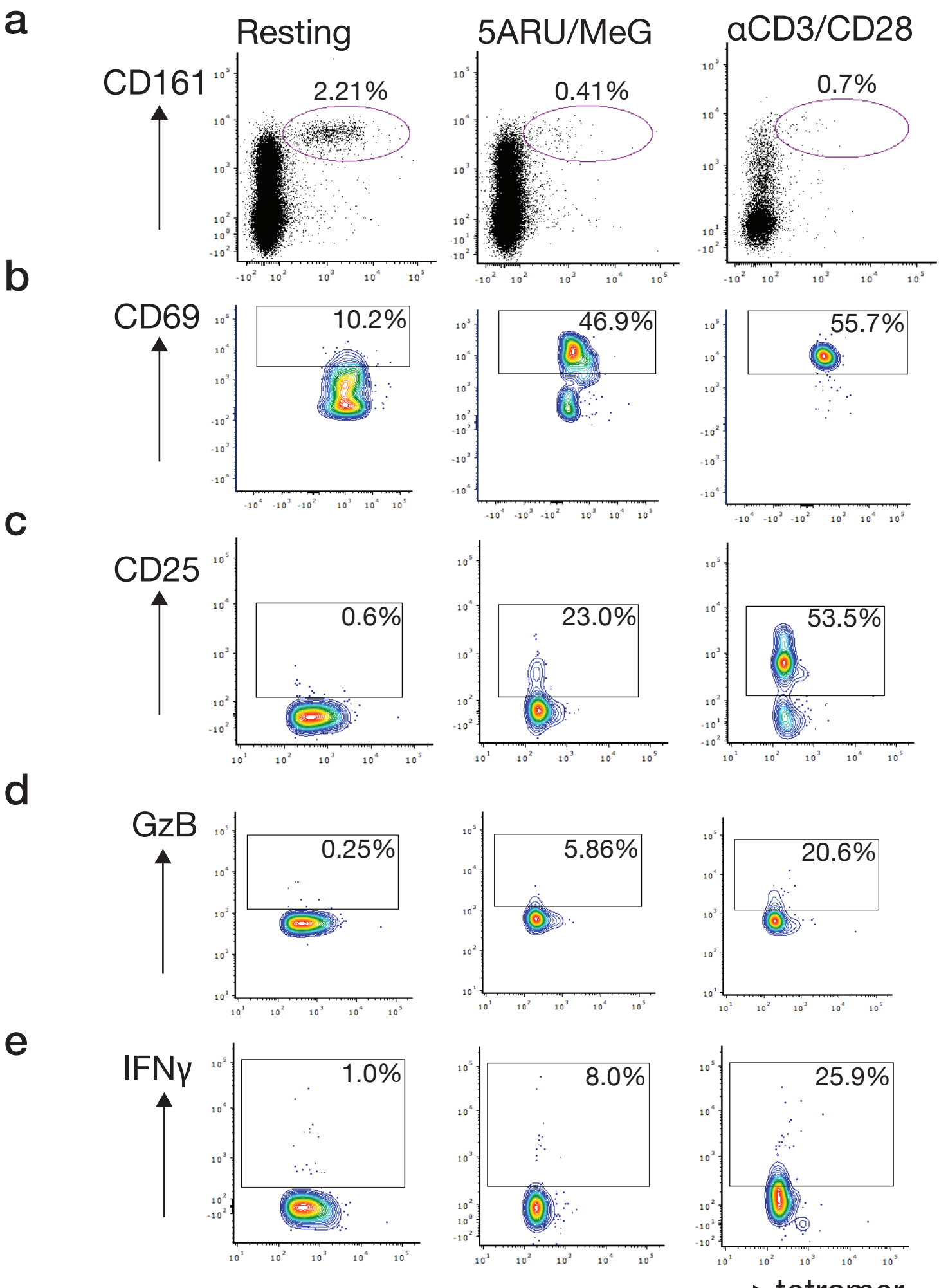
a
Resting
5ARU/MeG
αCD3/CD28
CD161
2.21%
0.41%
0.7%
b
CD69
10.2%
46.9%
55.7%
c
CD25
0.6%
23.0%
53.5%
d
GzB
0.25%
5.86%
20.6%
e
IFNγ
1.0%
8.0%
25.9%
tetramer

Figure S4

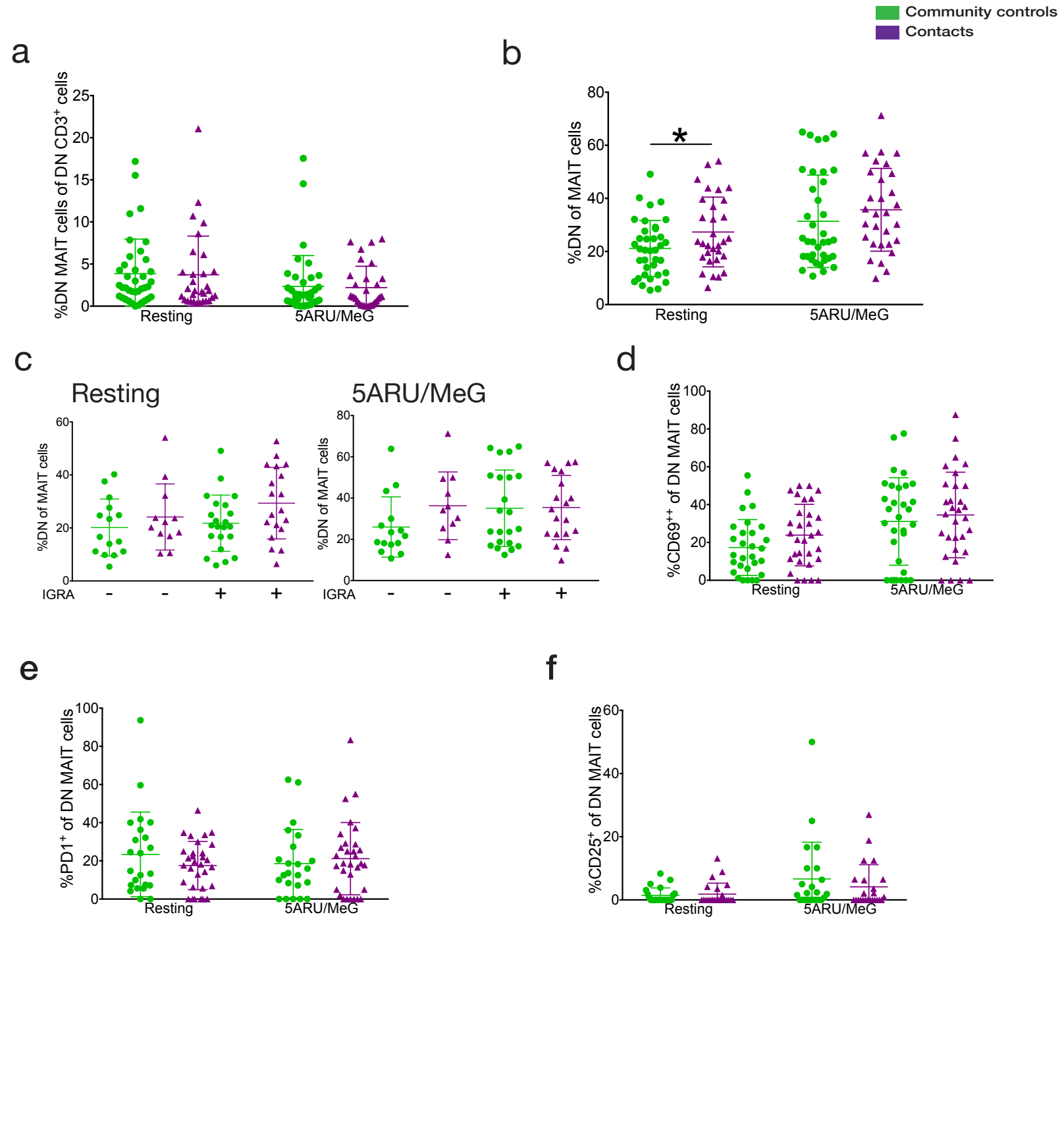
Community controls
Contacts
a
%DN MAIT cells of DN CD3+ cells
Resting
5ARU/MeG
b
%DN of MAIT cells
*
Resting
5ARU/MeG
c
Resting
5ARU/MeG
%DN of MAIT cells
IGRA
d
%CD69++ of DN MAIT cells
Resting
5ARU/MeG
e
%PD1+ of DN MAIT cells
Resting
5ARU/MeG
f
%CD25+ of DN MAIT cells
Resting
5ARU/MeG

Figure S5

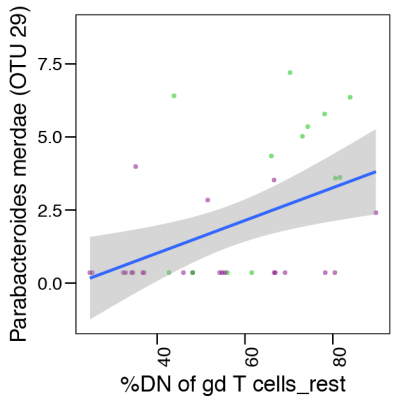

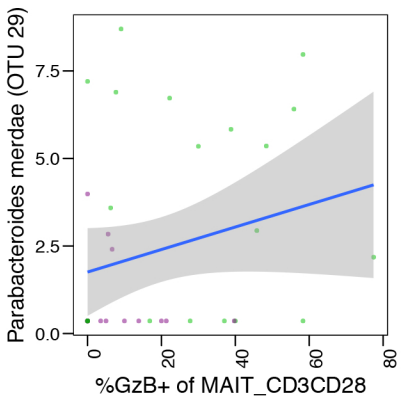

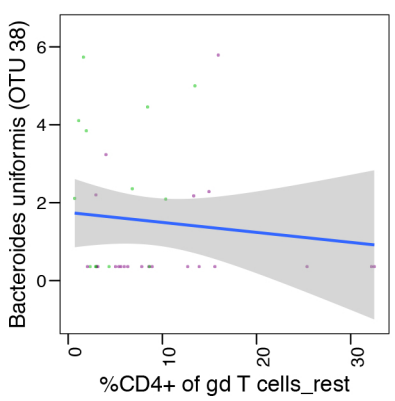

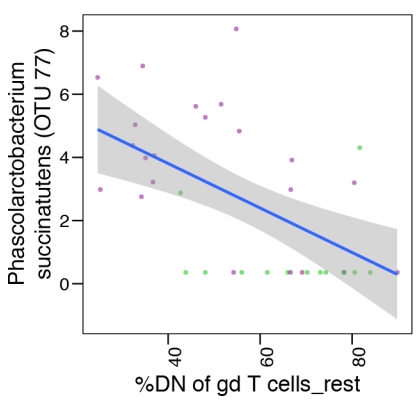

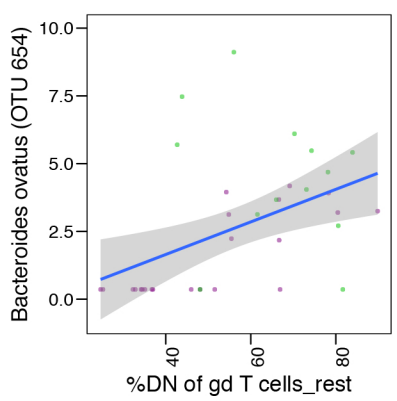

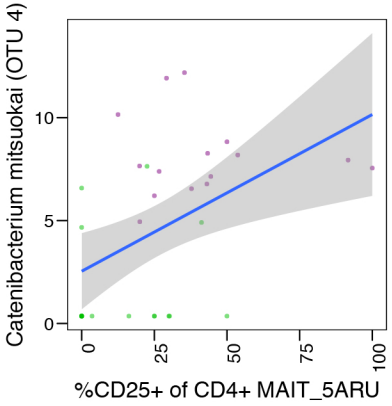

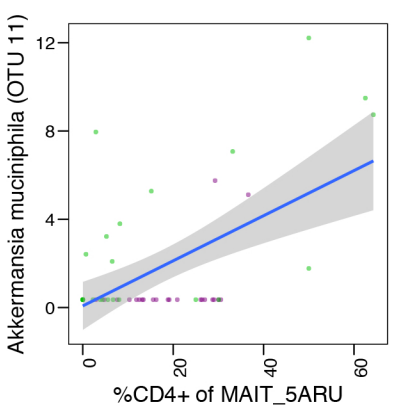

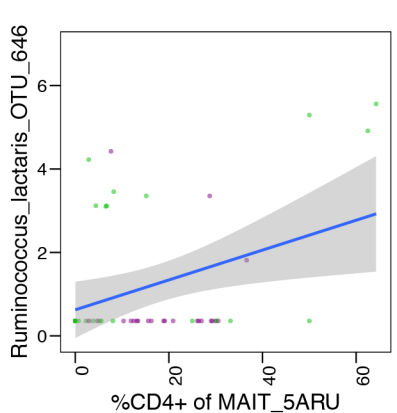

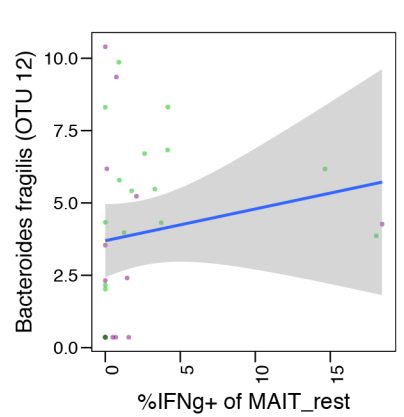

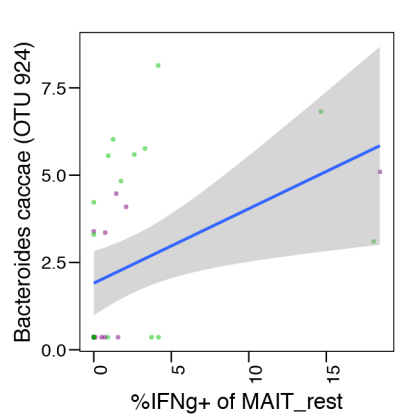

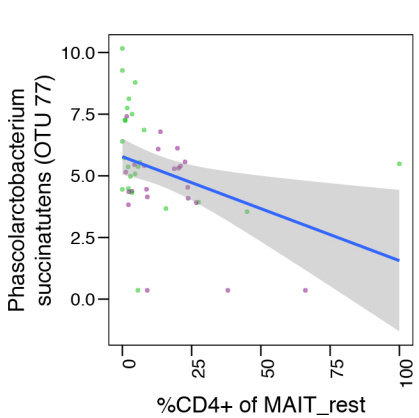

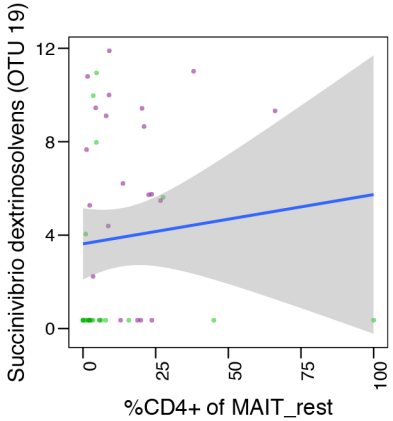

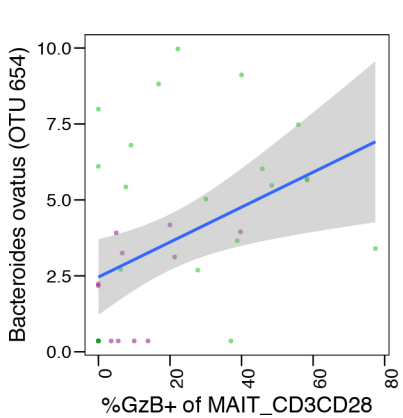

family contact
community control

Figure S6